Journal of Solid State Chemistry **147,** 358–365 (1999)
Article ID jssc.1999.8338, available online at http://www.idealibrary.com on IDEAL®

Trinegative $[Re_6S_7Br_7]^{3-}$ Anionic Cluster Unit Synthesized via Direct High-Temperature Route in the Quaternary System *M*–Re–S–Br (*M* = Alkaline) and Its Tetrahydrate $Rb_3[Re_6S_7Br_7]\cdot 4H_2O$

A. Slougui, A. Perrin,[1] and M. Sergent

Laboratoire de Chimie du Solide et Inorganique Moléculaire, UMR CNRS 6511, Université de Rennes 1, Campus de Beaulieu,
Avenue du Général Leclerc, 35042 Rennes Cédex, France

Received December 24, 1998; in revised form March 11, 1999; accepted April 21, 1999

A trivalent cluster unit has been synthesized by the solid-state route for the first time in the Rb–Re–S–Br system. The new rhombohedral compound $Rb_3Re_6S_7Br_7$ is built from octahedral Re_6 clusters surrounded by two μ_3-S^i and six μ_3-L^i ligands in which L^i acts as $\frac{1}{6}$Br + $\frac{5}{6}$S. These L^i ligands exhibit a rotational disorder. The stacking and environments in this structure are very comparable to those of the tetravalent cluster unit in $Rb_5Re_6S_8Br_6$, Br. Acetone solutions of $Rb_3Re_6S_7Br_7$, when evaporated in air, deposit crystals of the triclinic tetrahydrate $Rb_3Re_6S_7Br_7\cdot 4H_2O$ which is in thermodynamic equilibrium with the anhydrous salt.

Key Words: **clusters; rhenium; thiobromides; crystal structure.**

I. INTRODUCTION

The chemistry of Re_6L_{14} units based on the Re(III) octahedral cluster is now well documented. Beside a number of ternary sulfides (selenides) reported by Bronger's group (1), a wide variety of chalcohalides have been obtained via high-temperature synthesis and structurally characterized (2–6). They include both neutral units [isolated or halogen bridged in one, two, or three directions of the space (3, 4)] or anionic entities. Well-known examples are the cubic compounds $M^{I}Re_6Se_5Cl_9$ (5) and $M^{II}Re_6Se_6Cl_8$ (6), based on monoanionic and dianionic units, respectively, and the tetravalent $[Re_6Se_8Cl_6]^{4-}$ anion (7).

Up to very recently, the trivalent anionic salt was still missing. In fact, it is expected that $Rb_{2.5}[Re_6S_{6.5}Cl_{7.5}]$ contains a mixture of divalent and trivalent anionic units (8), but of course, it was not possible to isolate a trivalent unit in this compound. $(PPh_4)_3[Re_6S_7Br_7]$ has been reported (9), but was formed by a two-step quite low temperature reaction, not by direct synthesis. Very recently, we became aware of the synthesis of $Cs_3Re_6S_7Cl_7$ (10) obtained via a solid-state chemistry route.

The brominated analogues are not always isostructural with the chlorinated ones. One relevant example is given by the monoclinic structure of $KRe_6S_5Br_9$ where the K^+ ion is in a Br_6 prismatic environment (11), whereas in the cubic parent $KRe_6Se_5Cl_9$, it lies in a Cl_6 octahedron (5).

In this paper, we report the *ab initio* synthesis by the direct high-temperature route of $Rb_3Re_6S_7Br_7$ and we describe the crystal structure of this new cluster compound and of its tetrahydrate $Rb_3Re_6S_7Br_7\cdot 4H_2O$.

II. EXPERIMENTAL

1. *Synthesis*

High-temperature syntheses were carried out from RbBr and elemental Re, S, and Br_2. RbBr (92 mg), Re (207 mg) and S (42 mg) were weighed and mixed together and transferred in a silica tube (about 2500 mm^3) in a glove box. Liquid bromine (about 60 mg) was then added under an argon atmosphere and frozen in liquid nitrogen before sealing the tube under a vacuum (10^{-1}–10^{-2} Torr of argon residual atmosphere).

The tubes were fired in a vertical furnace at temperatures in the range 800–1000°C for periods between 40 and 160 h. The synthesis temperature was typically reached in 4 h. After the reaction, the furnace was switched off and allowed to cool naturally down to room temperature in about 3 h.

The hydrated salt was obtained by dissolution of the former compound (150 mg) in acetone (30 ml) and air-atmosphere evaporation of the solution at room temperature.

2. *Structural Data*

X-ray diffraction patterns were recorded with an Inel CPS 120 localization detector diffractometer working

---

[1] To whom correspondence should be addressed. E-mail: aperrin@univ-rennes1.fr. Fax: +(33) 2.99.63.57.04.

0022-4596/99 $30.00

with Cu$K\alpha_1$ radiation. Silicium was used as an internal standard.

Due to the existence of a number of volatile phases at the synthesis temperature, single crystals suitable for X-ray data collection were directly grown during the high-temperature synthesis (850°C, 70 h) of $Rb_3Re_6S_7Br_7$ by endogen chemical vapor transport. Well-formed, dark red octahedral or broad needle-shaped crystals of $Rb_3Re_6S_7Br_7 \cdot 4H_2O$ were obtained by solvent evaporation. Data were collected using a CAD-4 Nonius diffractometer under the conditions summarized in Tables 1 and 2. Unit-cell constants were refined from 25 reflections. The structures were solved by the direct method and Fourier analysis and refined using Molen programs. Anionic disorder was accounted for by refining the multiplicity of a pseudoatom defined as $L = \frac{7}{8}S + \frac{1}{8}Br$ (DISORDER program) with the average diffusion factor $f_L = \frac{7}{8} f_S + \frac{1}{8} f_{Br}$ (corresponding to 38 electons per pseudoatom). So, a refined multiplicity larger than the site multiplicity means only that the bromine concentration is larger than $\frac{1}{8}$. The S/Br ratio was then calculated from the experimental number of electons per site, assuming $S + Br = 1$. Full occupancy of Br^a and Rb positions was checked for. A ψScan empirical absorption correction was used.

TABLE 1
Crystal Data and Experimental Parameters for the Intensity Data Collection for $Rb_3Re_6S_7Br_7$ Compound

I. Crystal data

Formula: $Rb_3Re_6S_7Br_7$
$M = 2157.43$ g/mol
Crystal system: trigonal
Space group: $R\bar{3}c$ (No. 167)
$a_h = 15.335$ (1) Å, $c_h = 18.564$ (2) Å
$V = 3779.8$ (5) Å^3
$a_R = 10.8010$ (4) Å, $\alpha_R = 90.448$ (6)°
Unit cell refined from 25 reflections (6° $< \theta <$ 19°)
$\rho_{cal} = 5.69$ g/cm^3
$Z = 6$
Crystal size: $0.04 \times 0.02 \times 0.08$ mm^3
Linear absorption factor: 46.27 mm^{-1}

II. Data collection

Temperature: 295 K
Wavelength: Mo$K\alpha_1$
Enraf Nonius CAD-4
Scan mode: ω–2θ
Monochromator: graphite
θ_{max}: 35°
$0 < h < 24$, $0 < k < 24$, $-29 < l < 29$
4015 measured reflections
1681 independent reflections with $I > \sigma(I)$
R_{int}: 0.032

III. Structure determination

Lorentz and polarization corrections
Absorption correction: ψScan from 3 reflections
Refinement on F
39 refined parameters
616 independent reflections with $I > 3\sigma(I)$
Unweighted agreement factor $R = 0.031$
Weighted agreement factor $R_\omega = 0.032$ $\quad \omega = 4F_o^2/[\sigma^2(F_o^2) + (0.03\,F_o^2)^2]$
Goodness of fit: $S = 0.884$
$\Delta\rho$ max $= 0.66\ e^-$ Å^{-3}
$(\Delta/\sigma)_{max} < 0.02$
Extinction coefficient: $5.0(3) \times 10^{-8}$

TABLE 2
Crystal Data and Experimental Parameters for the Intensity Data Collection for $Rb_3Re_6S_7Br_7 \cdot 4H_2O$

I. Crystal data

Formula: $Rb_3Re_6S_7Br_7 \cdot 4H_2O$
$M = 2229.4$ g/mol
Crystal system: triclinic
Space group: $P\bar{1}$ (No. 2)
$a = 9.54$ (1) Å, $b = 9.62$ (2) Å,
$V = 1446(5)$ Å^3
$c = 17.72$ (3) Å, $\alpha = 82.7$ (1)°,
$\beta = 82.1$ (1)°, $\gamma = 64.2$ (2)°
Unit cell refined from 25 reflections (6° $< \theta <$ 15°)
$\rho_{cal} = 5.1$ g/cm^3
$Z = 2$
Crystal size: $0.08 \times 0.03 \times 0.12$ mm^3
Linear absorption factor: 40.32 mm^{-1}

II. Data collection

Temperature: 295 K
Wavelength: Mo$K\alpha_1$
Enraf Nonius CAD-4
Scan mode: ω–2θ
Monochromator: graphite
θ_{max}: 30°
$-13 < h < 13$, $0 < k < 13$, $-24 < l < 24$
8856 measured reflections
8391 independent reflections with $I > \sigma(I)$
R_{int}: 0.056

III. Structure determination

Lorentz and polarization corrections
Absorption correction: ψScan from 3 reflections
Refinement on F
263 refined parameters
4503 independent reflections with $I > 5\sigma(I)$
Unweighted agreement factor $R = 0.05$
Weighted agreement factor $R_w = 0.06$ $\quad \omega = 4F_o^2/[\sigma^2(F_o^2) + (0.05\,F_o^2)^2]$
Goodness of fit: $S = 1.4$
$\Delta\rho$ max $= 2.3\ e^-$ Å^{-3}
$(\Delta/\sigma)_{max} < 0.05$

III. RESULTS

1. Phase Identification

A nearly single-phase material was obtained for synthesis temperature and time in the explored range. Only minute amounts of ReS_2 are often present. Increasing the Br/S ratio (and, of course, decreasing correlatively the Rb^+ concentration) leads to $Rb_2Re_6S_6Br_8$ (12), and, conversely, decreasing it leads to $Rb_5Re_6S_8Br_7$ (12). No indication of any composition range was evidenced for the new phase. Electron microprobe analyses of obtained crystals, using an Oxford-Link energy-dispersive spectrometer, gave results in agreement with the $Rb_3Re_6S_7Br_7$ formula within experimental error (calc.: $Rb_{0.13}Re_{0.26}S_{0.30}Br_{0.30}$, found: $Rb_{0.13}Re_{0.30}S_{0.29}Br_{0.27}$).

Crystals obtained by recrystallization from acetone solution of the previous material exhibited a fully distinct X-ray diffraction pattern. The Rb:Re:S:Br ratios, determined by energy-dispersive spectrometry (EDS) analysis were not significantly different. However, infrared spectra, recorded in the range 400–4000 cm^{-1}, displayed absorption bands characteristic of water molecules around 1620 cm^{-1} (bending mode) and 3200–3400 cm^{-1} (stretching modes).

2. *Crystal Structures*

2.1. Anhydrous $Rb_3Re_6S_7Br_7$ compound. $\mathrm{Rb_3[Re_6S_7Br_7]}$ crystallizes in the trigonal system with the unit-cell constants $a = 15.335(1)$ Å and $c = 18.564(2)$ Å. Systematic absences suggest the $R\bar{3}c$ space group (No. 167) and the corresponding rhombohedral unit-cell constants are $a = 10.8010(4)$ Å and $\alpha = 90.448(6)°$.

Atomic fractional coordinates and refined equivalent isotropic thermal factors are reported in Table 3 (13). Meaningful interatomic distances and angles are given in Table 4 (13).

The structure is built from $\mathrm{Rb^+}$ ions and $(|\mathrm{Re_6}L^{\mathrm{i}}_8|L^{\mathrm{a}}_6)^{3-}$ units [L^{i} = inner ligands, L^{a} = apical ligands according to the H. Schäfer notation (14)].

The $\mathrm{Re_6}$ cluster, centered on a $\bar{3}$ point position, is a quasi-perfect octahedron as shown by very near identical Re–Re distances as well as angles very close to 60° and 90°. The structurally independent metal–metal distances (2.593 and 2.602 Å) are hardly significantly different and are in very good agreement with the assumption of a Pauling bond order (PBO) value of unity for each of the 12 Re–Re bonds (3, 15). That means consequently a valence electron concentration (VEC) equal to 24, in good agreement with the red color and the insulating character of the crystals.

Similarly, the $\mathrm{Re_6}L^{\mathrm{i}}_8$ unit appears very regular although formed by two different types of ligands: as shown in Table 5, $L(1)$ atoms are pure sulfur whereas $L(2)$ positions are occupied by both sulfur and bromine, giving for the $\mathrm{Re_6}L^{\mathrm{i}}_8$ core the composition $\mathrm{Re_6[(S^i)_2(S^i_{0.81}Br^i_{0.19})_6]}$. Such a full occupancy of the two apices of the L^{i}_8 cube by pure sulfur means a partial ordering of the ligands: a similar result was reported in the example of the ternary rhenium thiobromide $\mathrm{Re_6S_7Br_4}$ (6). In $\mathrm{(PPh_4)_3[Re_6S_7Br_7]}$ also, the L^{i}_8 positions present an uneven statistical distribution (9).

The $\mathrm{Re_6}L_{14}$ unit is completed by six apical bromines (fully occupied positions), leading to the usual geometry depicted in Fig. 1. The Re–Br$^{\mathrm{a}}$ distance, 2.555 Å, is clearly inbetween the values observed for univalent (and divalent) units and tetravalent units in a variety of thiobromides. Figure 2 summarizes a number of data (12) and it is clearly observed that $\mathrm{Rb_3Re_6S_7Br_7}$ follows the general trend: when the anionic charge increases, $\mathrm{(Br^a)^-}$ ions are more strongly repelled by coulombic interactions with the $\mathrm{Re_6}L_8$ core, and then the Re–Br$^{\mathrm{a}}$ distances increase. Similar behavior has been also reported in the examples of ternary and quaternary rhenium thiochlorides (8).

Figure 3 schematically represents the unit cell (in the trigonal setting) where only the $\mathrm{Re_6}$ clusters and $\mathrm{Rb^+}$ ions have been drawn for clarity. Due to the 3_1 screw axis, a sequential stacking $ABB'A'B''B'''$ is observed.

As shown in Fig. 4, the environment of the rubidium ion is quite complex: it lies on a (18*e*) Wyckoff position and is surrounded by two Br$^{\mathrm{a}}$, one L^{i}, and one S which are then doubled by the twofold axis effect. The Rb–Br$^{\mathrm{a}}$, Rb–S, and Rb–L^{i} distances are heterogeneous and, while the Re–S distance is close to the sum of ionic radii, one Re–Br

TABLE 3
Positional Parameters and Equivalent Isotropic Thermal Factors for $\mathrm{Rb_3Re_6S_7Br_7}$

Atom	*x*	*y*	*z*	*B* (Å^2)
Re	0.90530(4)	0.00559(4)	0.05733(3)	1.72(1)
L(1)	0	0	0.6589(4)	2.21(9)
L(2)	0.3225(3)	0.4715(3)	0.6133(2)	3.24(8)
Br	0.4474(1)	0.3444(1)	0.47940(8)	3.10(4)
Rb	0.1977(2)	0	0.250	5.44(9)

TABLE 4
Interatomic Distances (Å) and angles (°) for $\mathrm{Rb_3Re_6S_7Br_7}$

	$\mathrm{Re_6}$ cluster		
Re–Re	2.5925(9)	Re–Re–Re	60.00(2)
Re–Re	2.6017(8)		90.00(3)
Re–Re$^{\mathrm{i}}$	3.6729(9)		60.12(2)
			60.12(2)
			90.00(3)
			59.75(2)
	L_8 cube		
L(1)–*L*(2)	3.465(6)	*L*(1)–*L*(2)–*L*(2)	89.0(1)
L(2)–*L*(2)	3.476(5)	*L*(2)–*L*(2)–*L*(2)	90.8(1)
		L(2)–*L*(1)–*L*(2)	91.2(2)
	$(\mathrm{Re_6}L_8)\mathrm{Br_6}$ unit		
Re–*L*(1)	2.407(6)	*L*(1)–Re–*L*(2)	90.42(8)
Re–*L*(2)	2.479(3)	*L*(2)–Re–*L*(2)	89.5(1)
Re–*L*(2)	2.475(5)	*L*(2)–Re–*L*(2)	89.4(1)
Re–*L*(2)	2.463(4)	*L*(2)–Re–*L*(1)	90.34(9)
Re–Br	2.555(2)		
	Rubidium environment		
Rb–Br	3.377(3) × 2		
Rb–*L*(1)	3.472(4) × 2		
Rb–*L*(2)	3.657(4) × 2		
Rb–Br	3.687(2) × 2		

TABLE 5
Refined Multiplicities for $\mathrm{Rb_3Re_6S_7Br_7}$^{a}

Refined atom	Position	Site multiplicity	Refined multiplicity	Atomic occupancy
L(1)	12*c*	0.333	0.283(4)	1S
L(2)	36*f*	1	1.068(9)	0.19Br + 0.81S
Rb	18*e*	0.5	0.501(3)	1Rb

$^a f_{\mathrm{L}} = \frac{7}{8} f_{\mathrm{S}} + \frac{1}{8} f_{\mathrm{Br}}$.

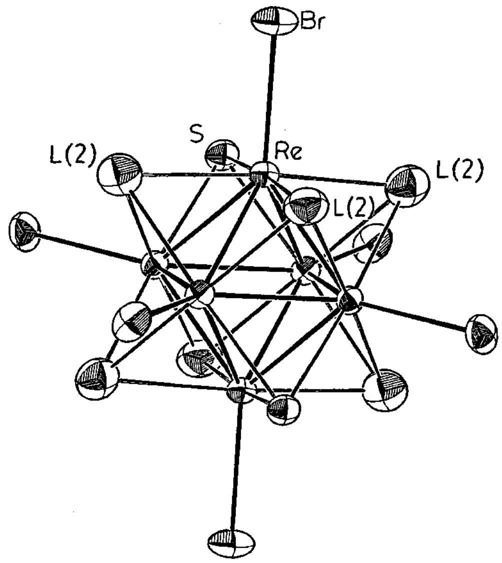

FIG. 1. Anionic unit $|\mathrm{Re_6S_7Br}|\mathrm{Br}_6^{a\,3-}$ (thermal ellipsoids at 50% probability).

distance is shorter and both the second one and the Re–L distances are longer than the ideal values. The second sphere of coordination is a pseudotetrahedron of Re_6L_{14} units as shown in Fig. 4.

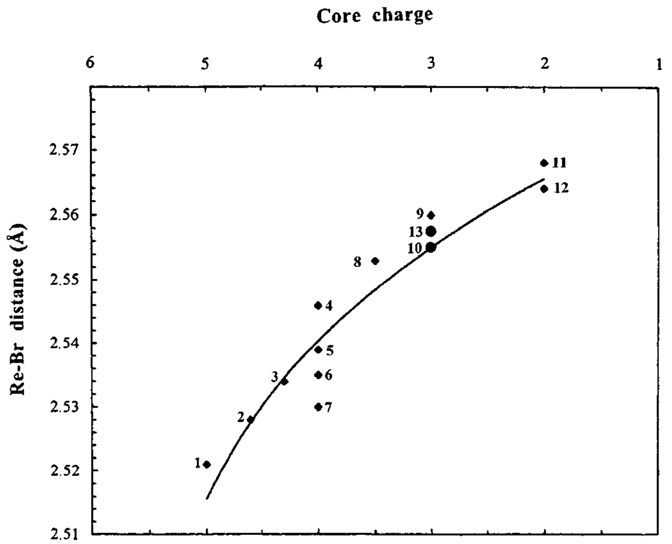

FIG. 2. Correlation (the line is only a guide for the eye) between the distance Re–Br^a and the charge of the anionic unit (i.e., correlatively the $|Re_6L^i_8|^{n+}$ core charge) for a number of thiobromides (12). (1) $KRe_6S_5Br_9$, (2) $Cd_{0.7}Re_6S_{5.4}Br_{8.6}$, (3) $KRe_6S_{5.7}Br_{8.3}$, (4) $Ag_2Re_6S_6Br_8$, (5) $Ag_{0.5}K_{1.5}Re_6S_6Br_8$, (6) $Cs_2Re_6S_6Br_8$, (7) $Rb_2Re_6S_6Br_8$, (8) $K_{2.5}Re_6S_{6.5}Br_{7.5}$, (9) $Cs_3Re_6S_7Br_7$, (10) $Rb_3Re_6S_7Br_7$, (11) $Rb_5Re_6S_8Br_7$, (12) $Cs_4KRe_6S_8Br_7$, (13) $Rb_3Re_6S_7Br_7{\cdot}4H_2O$.

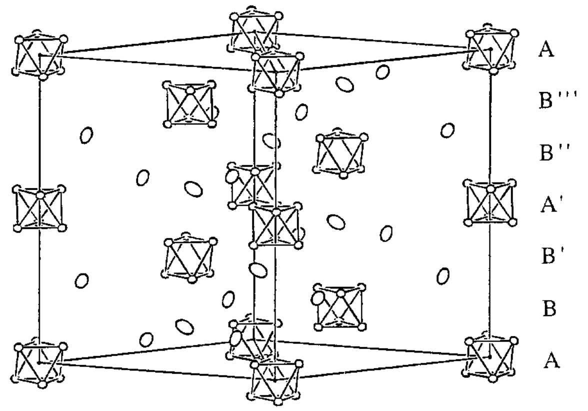

FIG. 3. Unit cell of $Rb_3Re_6S_7Br_7$ drawn in the hexagonal setting. All the ligands have been omitted for clarity.

2.2. Tetrahydrate $Rb_3Re_6S_7Br_7{\cdot}4H_2O$. The structure of the tetrahydrate is clearly different from that of the pristine salt, as the symmetry is now triclinic. The unit-cell constants are given in Table 2 together with the data collection and the refinement conditions. Atomic fractional coordinates and refined equivalent isotropic thermal factors are reported in Table 6 (13). Meaningful interatomic distances are given in Table 7 (16) and refined statistical occupancies in Table 8.

The unit cell contains two independent cluster units, six rubidium ions, and eight oxygens attributed to water molecules. The asymmetric unit is built from two half-cluster units corresponding to Re(1)–(3), *L*(1)–(4), Br(1)–(3) for the unit denoted I and Re(4)–(6), *L*(5)–(8), Br(4)–(6) for unit II, and centered on the 000 and $00\frac{1}{2}$ inversion centers. A simplified representation of the unit cell is given Fig. 5.

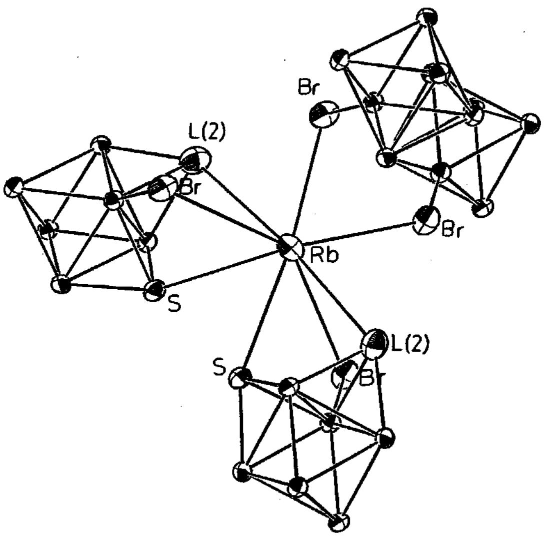

FIG. 4. Environment of the Rb^+ cation in $Rb_3Re_6S_7Br_7$.

Although the symmetry is low, the units are hardly distorted: as an example, the Re–Re distances lie in the range 2.595–2.601 Å for cluster I and 2.586–2.608 Å for cluster II. The average values, 2.598 and 2.596 Å for the first and second clusters, respectively, are, as previously, in full agreement with the assumption of order one metal–metal bonds. Also, the Re–L^i distances show only a quite narrow distribution. The Re–Br^a distances, 2.557 Å on average, are very close to that observed in the anhydrous compound (2.555 Å), confirming the presence of a trivalent anionic unit.

The eight inner ligands are disordered, but in each unit, six of them are pure or nearly pure sulfur. The actual distribution is wide when compared with that of the anhydrous material, but, in the latter case, symmetry effects in fact averaged the observed values.

As previously, the environment of the rubidium countercations is very complex and, in addition, is strongly different for each of the three independent cations of the structure. A significant difference with the anhydrous compound is the presence, in the first shell of coordination of each rubidium, of at least one oxygen atom (water molecule) at a short distance, 2.84–2.88 Å: the sum of the ionic radius of Rb^+ and the crystal radius of oxygen is 2.84 Å (17), in close agreement with the observed distances.

TABLE 6
Positional Parameters and Equivalent Isotropic Thermal Factors for $Rb_3Re_6S_7Br_7 \cdot 4H_2O$

Atom	*x*	*y*	*z*	*B* (Å^2)
Re(1)	0.0192(1)	– 0.1224(1)	0.09008(6)	1.12(2)
Re(2)	0.2136(1)	– 0.0805(1)	– 0.01813(6)	1.10(2)
Re(3)	0.9986(1)	– 0.15429(9)	– 0.05082(6)	1.11(2)
Re(4)	0.14919(9)	0.85888(9)	0.43711(6)	0.99(2)
Re(5)	0.04034(9)	0.15684(9)	0.44633(6)	0.99(2)
Re(6)	0.15014(9)	0.96672(9)	0.56335(6)	0.99(2)
Br(1)	0.0388(3)	0.7108(3)	0.2162(2)	2.65(6)
Br(2)	0.4896(3)	0.1905(3)	0.0469(2)	2.36(6)
Br(3)	0.9956(3)	0.6295(3)	0.8801(2)	2.64(6)
Br(4)	0.3640(3)	0.6561(3)	0.3557(2)	2.55(6)
Br(5)	0.0977(3)	0.3762(3)	0.3740(2)	2.31(6)
Br(6)	0.3671(3)	0.9118(3)	0.6489(2)	2.26(5)
L(1)	0.2219(6)	0.6576(5)	0.0208(3)	2.0(1)
L(2)	0.1799(7)	0.8950(6)	0.8533(4)	1.8(1)
L(3)	0.2202(6)	0.9534(6)	0.1146(4)	1.3(1)
L(4)	0.1820(6)	0.1852(6)	0.9467(4)	2.1(1)
L(5)	0.0390(4)	0.0457(4)	0.3222(3)	2.07(8)
L(6)	0.2379(6)	0.6957(6)	0.5491(4)	1.9(1)
L(7)	0.0389(7)	0.2424(6)	0.5675(4)	2.0(1)
L(8)	0.3122(6)	0.9858(6)	0.4500(4)	1.9(1)
Rb(1)	0.3616(4)	0.3282(4)	0.5022(2)	3.96(8)
Rb(2)	0.4261(5)	0.4368(4)	0.1934(3)	4.8(1)
Rb(3)	0.4383(6)	0.1245(5)	0.7836(3)	5.4(1)
O(1)	0.319(2)	0.183(3)	0.229(1)	6.3(6)
O(2)	0.278(3)	0.605(3)	0.734(1)	7.6(8)
O(3)	0.409(3)	0.382(2)	0.876(1)	5.1(6)
O(4)	0.276(2)	0.340(2)	0.662(2)	9.4(7)

TABLE 7
Significant Interatomic Distances (Å) for $Rb_3Re_6S_7Br_7 \cdot 4H_2O$

Re_6 clusters			
Re(1)–Re(2)	2.599(1)	Re(4)–Re(5)	2.608(1)
Re(1)–Re(3)	2.598(1)	Re(4)–Re(6)	2.586(1)
Re(2)–Re(3)	2.597(1)	Re(5)–Re(6)	2.589(1)
Re(1)–Re(2)^i	2.596(1)	Re(4)–Re(5)^i	2.587(1)
Re(1)–Re(3)^i	2.601(1)	Re(4)–Re(6)^i	2.608(1)
Re(2)–Re(3)^i	2.595(1)	Re(5)–Re(6)^i	2.601(1)
Re(1)–Re(1)^i	3.678(1)	Re(4)–Re(4)^i	3.676(1)
Re(2)–Re(2)^i	3.668(1)	Re(5)–Re(5)^i	3.671(1)
Re(3)–Re(3)^i	3.675(1)	Re(6)–Re(6)^i	3.670(1)
$(Re_6L_8)Br_6$ units			
$\langle Re\text{–}L_j \rangle$ $j = 1\text{–}4$	2.442	$\langle Re\text{–}L_j \rangle$ $j = 5\text{–}8$	2.436
Re(1)–Br(1)	2.559(3)	Re(4)–Br(4)	2.552(3)
Re(2)–Br(2)	2.556(3)	Re(5)–Br(5)	2.553(3)
Re(3)–Br(3)	2.557(3)	Re(6)–Br(6)	2.563(3)
Rubidium environment			
Rb(1)–O(1)	2.84(3)		
Rb(1)–*L*(8)	3.379(6)		
Rb(1)–*L*(6)	3.381(7)		
Rb(1)–Br(5)	3.467(5)		
Rb(1)–*L*(7)	3.534(8)		
Rb(1)–Br(6)	3.697(4)		
Rb(1)–*L*(6)	3.717(7)		
Rb(1)–*L*(8)	3.765(8)		
Rb(1)–Br(4)	3.829(5)		
Rb(2)–O(2)	2.89(3)		
Rb(2)–O(3)	3.00(3)		
Rb(2)–O(4)	3.11(3)		
Rb(2)–Br(1)	3.486(4)		
Rb(2)–Br(2)	3.551(6)		
Rb(2)–Br(4)	3.613(6)		
Rb(3)–O(3)	2.87(2)		
Rb(3)–O(1)	2.88(2)		
Rb(3)–O(2)	3.03(2)		
Rb(3)–*L*(4)	3.452(8)		
Rb(3)–Br(6)	3.641(7)		
Rb(3)–*L*(3)	3.684(8)		

The environment of the oxygen atoms is quite complex. The shortest distances are observed with rubidium ions [two for O(1) to O(3), and only one in the case of O(4)], as stated above, and with both Br^a and L^i ligands. The latter distances are in the range 3.3–3.5 Å and are clearly compatible with the formation of weak hydrogen bonds with these ligands: the O...Br and O...S distances, when hydrogen bonding is involved, are usually about 3.28 and 3.31 Å, respectively (18).

From both infrared spectra and Fourier difference residuals it is concluded that no solvent molecule is present in the tetrahydrate.

IV. DISCUSSION

$Rb_3Re_6S_7Br_7$ is the first example of a trivalent anionic unit in the quaternary systems *M*–Re–S–Br (*M* = alkaline).

TABLE 8
Refined Multiplicities for $Rb_3Re_6S_7Br_7 \cdot 4H_2O$[a]

Refined atom	Position	Site multiplicity	Refined multiplicity	Atomic occupancy
L(1)	2*i*	1	1.07(2)	0.19Br + 0.81S
L(2)	2*i*	1	0.91(1)	0.04Br + 0.96S
L(3)	2*i*	1	0.84(1)	1S
L(4)	2*i*	1	0.96(2)	0.09Br + 0.91S
L(5)	2*i*	1	1.44(2)	0.55Br + 0.45S
L(6)	2*i*	1	0.89(1)	0.01Br + 0.99S
L(7)	2*i*	1	0.92(2)	0.05Br + 0.95S
L(8)	2*i*	1	0.91(1)	0.04Br + 0.96S

[a] $f_L = \frac{7}{8} f_S + \frac{1}{8} f_{Br}$.

In fact, the trivalent anion seems to form only with quite large countercations: as an example, in a systematic study of these *M*–Re–S–Br systems, no evidence of any corresponding compound of the potassium was detected (12). On the other hand, $Cs_3Re_6S_7Br_7$ exists (12) but is not isostructural with the rubidium parent: it crystallizes in the monoclinic system ($P2_1/n$) with the following unit-cell constants: $a = 11.265(4)$ Å, $b = 13.148(6)$ Å, $c = 18.886(7)$ Å, $\beta = 106.81(3)°$. A special relationship between the unit-cell constant values leads to a systematic twinning of the crystals. However, the structure has been solved, at least in its major features. The anionic unit is similar to that of the Rb derivative, but the countercation environments are now very complex.

$Rb_3Re_6S_7Br_7$ is also very different from the corresponding $Cs_3Re_6S_7Cl_7$ recently reported by Guilbaud *et al.* (10). The latter is monoclinic, as the brominated compound, but crystallizes in the $P2_1/c$ space group. The unit cell contains two independent Cs^+ ions instead of one Rb in the structure of $Rb_3Re_6S_7Br_7$ and three Cs^+ in $Cs_3Re_6S_7Br_7$. Again, the environments of the cations are complex and difficult to describe as standard polyhedra.

In contrast, there is a close relationship between the structures of the trivalent $Rb_3Re_6S_7Br_7$ and the tetravalent $M_5Re_6S_8Br_6$,Br (12, 19, 20). These two compounds crystallize in the same system ($R\bar{3}c$) but with very different unit-cell constants [$a = 10.80$ Å, $\alpha = 90.44°$ and $a = 18.61$ Å, $\alpha = 30.53°$ (in the rhombohedral settings) for $Rb_3Re_6S_7Br_7$ and $Rb_5Re_6S_8Br_6$,Br (12), respectively]. A comparison of these two structures clearly reveals that the stacking and the orientation of the units are exactly the same, and, in addition, the environment of one Rb^+ cation [referred to as *M*(2) in (12, 19)] of the $Rb_5Re_6S_8Br_6$,Br structure is identical to that of Rb^+ in $Rb_3Re_6S_7Br_7$. The essential difference between the two structures is the strong elongation of the unit cell of the tetravalent unit-based compound: this is needed to gain enough extra space to accommodate the additional cations [referred as *M*(1)] as well as the extra bromine ion which is necessary to compensate the cationic charge excess.

$Rb_3Re_6S_7Br_7$ and its tetrahydrate are in thermodynamic equilibrium. For instance, at ambient temperature and

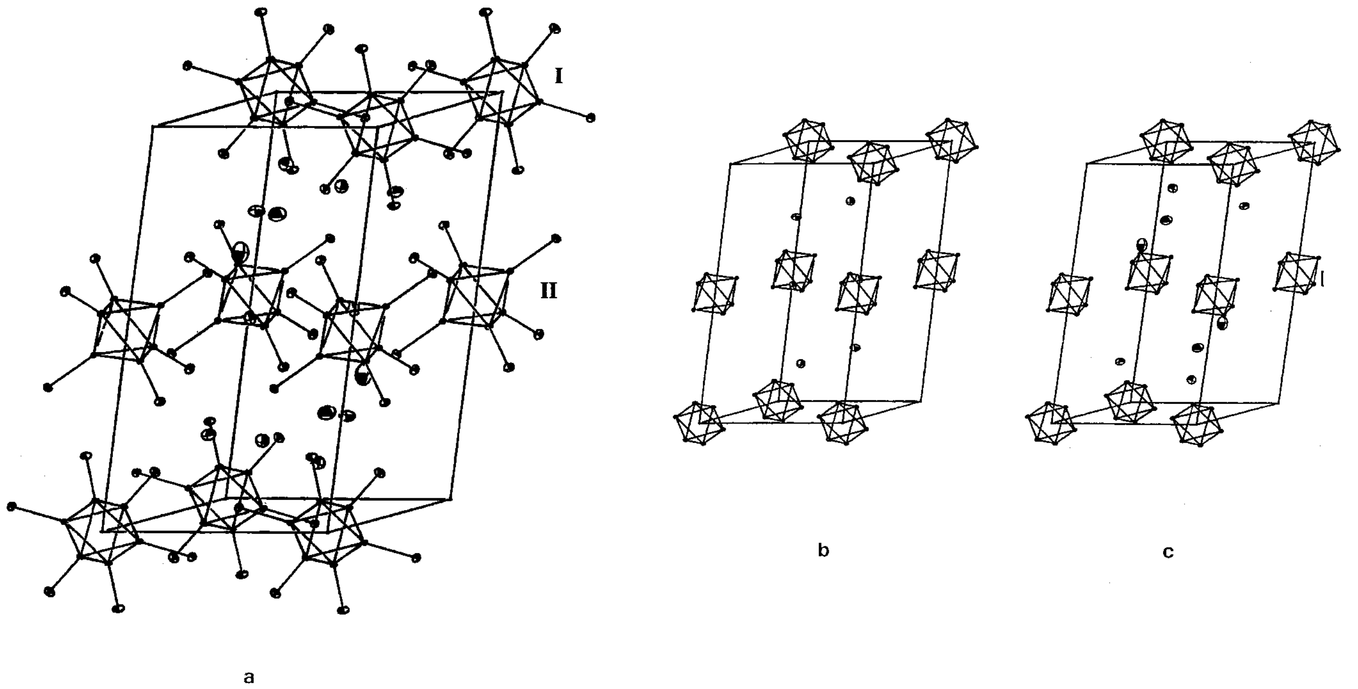

FIG. 5. Crystal structure of $Rb_3Re_6S_7Br_7 \cdot 4H_2O$ (two clusters omitted for clarity): (a) overall view (L^i ligands omitted for clarity), (b) representation reduced to the clusters and Rb^+ ions, (c) representation reduced to the clusters and oxygens of water molecules.

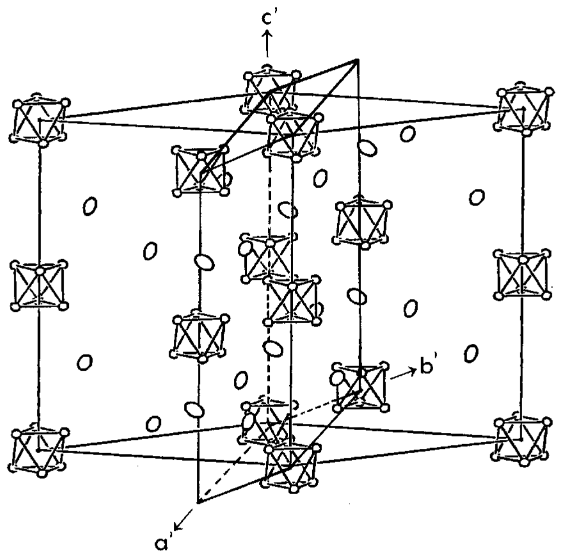

FIG. 6. Schematic representation of the pseudotriclinic unit cell reminiscent of the unit cell of the tetrahydrate, in the structure of the anhydrous $Rb_3Re_6S_7Br_7$.

for mild hygrometric conditions, $Rb_3Re_6S_7Br_7{\cdot}4H_2O$ returns to the anhydrous salt within a few weeks. Near 80°C, the dehydration takes only a few hours. The reverse reaction occurs when $Rb_3Re_6S_7Br_7$ is kept under saturated water vapor. Intermediate stages lead only to a mixture of the two compounds, so no subhydrate is expected to form, at least under the standard conditions reported above.

As the hydration–dehydration reaction occurs very easily under soft conditions and is perfectly reversible, a pseudotopotactic relation would be expected. Figure 6 schematically shows a possible relationship between the two structures: the pseudo unit cell

$$a' = 9.38\ \text{Å} \quad b' = 9.38\ \text{Å} \quad c' = 18.56\ \text{Å}$$

$$\alpha' = 70.74^\circ \quad \beta' = 109.68^\circ \quad \gamma' = 70.32^\circ$$

is reasonably close to the triclinic unit cell of the tetrahydrate and presents the same stacking of the cluster units, centered at 000 and $00\frac{1}{2}$ positions. The structural change from the anhydrous to the hydrated salt requires then some combined shifts along the common c directions and a small rotation of the clusters, which are expected to consume only a small energy.

Other information derived from comparison of the two structures reported here concerns the local arrangement of the anionic units. The latter appear to be built from seven sulfur and one bromine ligand because (i) this stoichiometry nearly fits the one derived from multiplicity refinements, (ii) these compounds are expected to be VEC24 compounds [a VEC23 octahedral cluster derivative has very recently been reported (21) but its formation requires electrochemical or chemical oxidation of the cluster in solution], and (iii) the possible disproportionation of the trivalent units as a mixture of divalent and tetravalent ones is ruled out by the normal orientation and size of the thermal ellipsoids of Br^a ligands (see, for instance, Fig. 1) as the Re–Br^a distance is strongly sensitive to the anionic charge of the unit (Fig. 2). Then the question is the distribution of the unique bromine ligand over the L^i_8 positions. In the case of $Rb_3Re_6S_7Br_7$, due to rhombohedral symmetry, the eight inner ligands split into two $12c$ and six $36f$ positions. It is clear that the bromine lies on one of the latter and the compound can be described on the basis of a statistic rotational disorder. $Rb_3Re_6S_7Br_7{\cdot}4H_2O$ is characterized by a lower symmetry, so the observed distribution more clearly represents the actual local structure.

Unit II in the structure illustrates this situation: six of the L^i_8 ligands are nearly pure S and the two remaining ones are half-occupied by S and Br ligands due to the inversion center. So the rotational distribution has been frozen, probably because all these ligands belong to the environment of one Rb^+ countercation. The situation is less marked for unit I for which it is worth noting that only two L^i ligands are coordinated to a cation.

ACKNOWLEDGMENTS

Dr. J. L. Adam is warmly acknowledged for recording infrared spectra and Dr. M. Potel for data collections and helpful discussions. Microprobe analyses were carried out in the CMEBA Center of the University of Rennes 1. This work has been supported in part by Fondation Langlois.

REFERENCES

1. W. Bronger, C. Koppe, and D. Schmitz, *Z. Anorg. Allgem. Chem.* **623,** 239 (1997).
2. A. Perrin and M. Sergent, *New J. Chem.* **12,** 337 (1988).
3. L. Leduc, A. Perrin, M. Sergent, J. C. Pilet, F. Le Traon, and A. Le Traon, *Mater. Lett.* **3,** 209 (1985).
4. A. Perrin, L. Leduc, and M. Sergent, *Eur. J. Solid State Inorg. Chem.* **28,** 919 (1991).
5. A. Perrin, L. Leduc, M. Potel, and M. Sergent, *Mater. Res. Bull.* **25,** 1227 (1990).
6. L. Leduc, Ph.D. dissertation, Rennes, 1983.
7. J. R. Long, A. S. Williamson, and R. H. Holm, *Angew. Chem. Int. Ed. Engl.* **34,** 226 (1995).
8. J. C. Gabriel, K. Boubekeur, and P. Batail, *Inorg. Chem.* **32,** 2894 (1993).
9. V. P. Fedin, H. Imoto, T. Saito, V. E. Fedorov, Y. V. Mironov, and S. Yarovoi, *Polyhedron* **15,** 1229 (1996).
10. C. Guilbaud, J. C. Gabriel, K. Boubekeur, and P. Batail, *C.R. Acad. Sci. Ser. C* **1,** 627 (1998).
11. A. Slougui, A. Perrin, and M. Sergent, *Acta Crystallogr. Sect. C* **48,** 1917 (1992).
12. A. Slougui, Ph.D. dissertation, Rennes, 1998.

13. Tables of anisotropic thermal factors and root mean square displacements are available on request.
14. H. Schäfer and H. G. von Schnering, *Angew. Chem.* **76,** 833 (1964).
15. L. Pauling, "The Nature of the Chemical Bond," 3rd ed. Cornell Univ. Press, Ithaca, NY, 1960.
16. Complete tables of distances and angles are available on request.
17. R. D. Shannon, *Acta Crystallogr. Sect. A* **32,** 751 (1973).
18. M. D. Joesten and L. J. Schaad, "Hydrogen Bonding." Marcel Dekker, New York, 1974.
19. A. Slougui, S. Ferron, A. Perrin, and M. Sergent, *Eur. J. Solid State Inorg. Chem.* **33,** 1001 (1996).
20. J. R. Long, L. S. Mc Carty, and R. H. Holm, *J. Am. Chem. Soc.* **118,** 4603 (1996).
21. C. Guilbaud, Ph.D. dissertation, Nantes, 1998.